Nanostructured Metal Oxides for Stoichiometric Degradation of Chemical Warfare Agents

Václav Štengl, Jiří Henych, Pavel Janoš, and Miroslav Skoumal

Contents

V. Štengl (✉) • J. Henych
Material Chemistry Department, Institute of Inorganic Chemistry AS CR v.v.i.,
250 68, Řež, Czech Republic
e-mail: stengl@iic.cas.cz

P. Janoš
Faculty of the Environment, University of Jan Evangelista Purkyně,
Králova Výšina 7, 400 96 Ústí nad Labem, Czech Republic

M. Skoumal
Military Institute, VeslaŘská 230, 637 00 Brno, Czech Republic

P. de Voogt (ed.), *Reviews of Environmental Contamination and Toxicology Volume 236*, Reviews of Environmental Contamination and Toxicology 236,
DOI 10.1007/978-3-319-20013-2_4

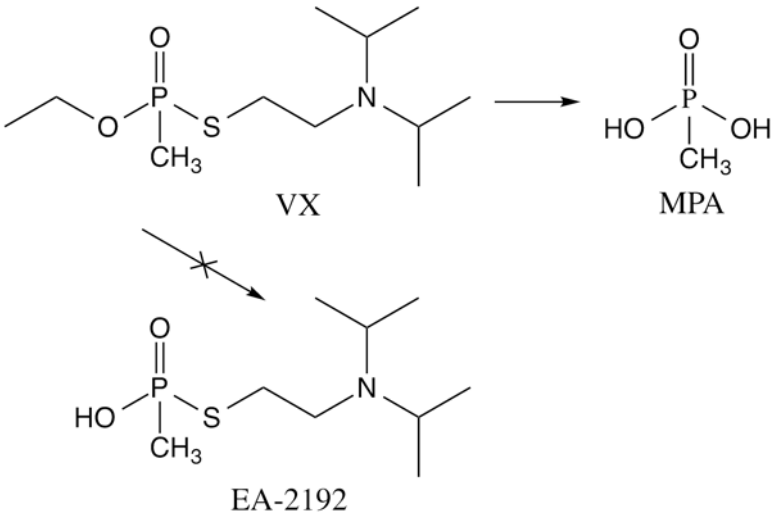

The nanostructure of reactive sorbents based on oxides of transient metals is crucial for degradation of chemical warfare agents

1 Introduction

Nerve agents (NA) are organic compounds (organophosphates) highly toxic to mammals. They are one of the most dangerous group of chemical warfare agents (CWAs) with rapid effects and penetration of the body by different entry routes. The chemically pure forms of G-agents, soman (O-pinacolyl methylphosphonofluoridate, GD), tabun (ethyl dimethylphosphoramidocyanidate, GA), sarin (*O*-isopropyl methylphosphonofluoridate, GB), and cyclosarin ((fluoro-methyl-phosphoryl) oxycyclohexane, GF) are colorless liquids with a water-like appearance, no noticeable odor, and are relatively soluble in both water and organic solvents. They possess high volatility, so the most likely pathway for substances to enter the body is the respiratory tract; the GD, GA, and GF can be regarded as contact hazards as well. V-agents, with VX as the main representative, are generally more persistent in the environment. In a chemically pure state, VX (O-ethyl S-[2-(diisopropylamino) ethyl] methylphosphonothioate) is a colourless liquid more viscous than water, with no noticeable odour. It has very low volatility and is poorly soluble in water, but highly soluble in organic solvents and fats. VR agent, as an isomer of VX, has very similar properties. Organophosphate compounds with a similar structure are known as effective pesticides (insecticides) in agriculture—parathion, parathion methyl, malathion, chlorpyrifos, dichlorvos, diazinon or fenitrothion belong to the most widely used and commonly available representatives of this group. Although their use has been restricted in many countries, some of them they are still applied in

great quantities and represent a potential threat to human health. Organophosphates are used also in industry as plasticizers or hydraulic fluids, or in medicine as therapeutics or compounds for researching nerve functions.

Finding effective and safe decontamination methods has long been of great concern for defense against chemical and biological warfare (CBW) agents (Yang et al. 1992). In the wake of new threats, such as terrorist attacks on civilian society, it has been recognized that decontamination and clean-up must meet more stringent criteria, which calls for new methods and materials and places new demands on operational procedures and appropriate risk analysis. Currently, decontamination procedures are characterized by intensive use of chemicals that themselves must be often treated with care, and they pose problems with regard to logistics, personnel, time and damage to equipment and to the environment. At the same time, the threat of a wider range of toxic chemicals, emerging from, for example, accidental or non-accidental industrial release, calls for broad-spectrum decontamination methods that can be efficiently deployed in urban areas. The use of nanostructured oxides as reactive sorbents for CWAs is anticipated, given the cost of sensitive components of military equipment (electronic devices, computers etc.).

Diverse physical, chemical and biochemical principles are employed in current decontamination strategies, such as adsorption, chemical reactions (mainly oxidation and nucleophilic substitution), enzymatic decomposition and others. Conventional adsorbents such as activated carbon, coal, alumina or clays, offer certain advantages such as low toxicity and low environmental risk, along with easy handling, long shelf life and relatively low cost as well. However, they are unable to destroy the toxic chemicals and thus require extensive and expensive post-decontamination treatment.

It was found that some sorption materials, typically metal oxides, are able not only to adsorb (physically) various toxic chemicals but also to break them down chemically into non-toxic (or less toxic) products. If the size of the individual oxide particles decreases to tens or even units of nanometers, an increase in their specific reactivity is observed. This acceleration of the heterogeneous reactions taking place on the surface of the nanocrystals is attributed mainly to an increase in the proportion of highly reactive sites such as edges and corners of crystals and in the number of dislocations and defects of shape. An increase in the surface area plays also a significant role—it follows from empirically obtained knowledge that increasing the specific surface area proportionally increases the observed rate of decomposition reactions. However, even a very substantial increase in the surface area itself can hardly explain the enhanced reactivity of nano-sized oxide materials. The reactivity of nanocrystalline metal oxides may be demonstrated by titanium oxide (Stengl et al. 2011a): In Fig. 1, a high-resolution transmission electron micrograph of nanocrystalline titanium dioxide presents a Ti4+ cation shown in white. The cations inside the crystal, which are not shown, have a coordination number of 6; the cations on the surface, shown in blue, have a coordination number of five; the cations on the edges, shown in red, have a coordination number of 4; finally, the cations in the corners, shown in green, have a coordination number of 3. Surface defect gaps (see arrow) also reduce the coordination number of surrounding ions. Generally, the

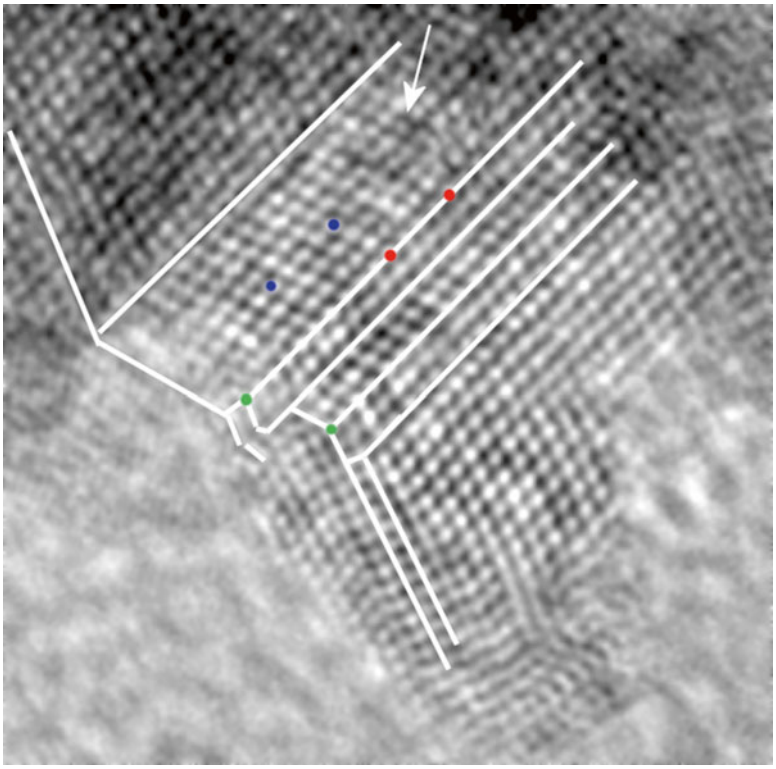

Fig. 1 The structure of a TiO_2 nanocrystal. Cations within the crystal (not shown) have a coordination number of 6, the cations on the surface (shown in *blue*) have a coordination number of 5, cations on the edges (shown in *red*) have a coordination number of 4, and cations in the corners (shown in *green*) have a coordination number of 3. Surface defect gaps (*arrow*) also reduce the coordination number of surrounding ions

lower the coordination number of cationic sites is, the higher is their reactivity (Sayle et al. 2008). This unique morphology of nanocrystals thus allows their high reactivity. It is assumed that the degradation of the chemical substance molecules occurs in two steps: the first is physical adsorption, and the second is chemical decomposition (Stark et al. 1996; Stark and Klabunde 1996).

In addition to the reactivity of the nanosized metal oxides, also other processes affecting the rate of conversion should be considered, namely the diffusion (external or internal) of substances to the active sites. As may be generalized from kinetic measurements, two stages with different kinetics may be distinguished on degradation curves (Stengl et al. 2011a): the initial stage characterized by a relatively rapid decrease in the concentration of the chemical agent is followed by a slower stage, where the decomposition rate is governed mainly by diffusion.

The first generation of nanostructured metal oxides was introduced by the Klabunde group in 1996 (Klabunde et al. 1996; Khaleel et al. 1999; Lucas et al. 2001;

Koper et al. 1997). Oxides of the alkaline earth elements, Al and Zn were the first representatives of the so- called reactive (ad)sorbents (the term "stoichiometric reagents" is used for this type of agent to distinguish them from "conventional" adsorbents). Reactive sorbents have been successfully used to destroy various types of CWAs (nerve agents sarin, soman and VX, as well as blistering agent HD). Their high degradation efficiency stems from their high surface area, porosity and nanocrystalline nature, which facilitates the formation of crystalline defects and other anomalies serving as reaction centers for chemical destruction. These types of nanocrystalline metal oxides were typically prepared from organic precursors using relatively laborious methods. More recently, some less expensive and environmentally friendly procedures have been developed to produce metal oxide- based reactive sorbents using simple and easily scalable "wet" synthetic routes. A wide range of new reactive sorbents with unique properties (extremely high surface area, high chemical reactivity and in some cases photocatalytic activity) has been introduced and tested for degradation of CWAs. Progress in this field during the last two decades is reviewed in this paper.

2 Nanostructured Oxides

2.1 Oxides of Alkaline Earth Metals

The nanostructured oxide of an alkaline earth metal, specifically MgO, with a particle size of 35 Å and a specific surface area of 1000 $m^2\ g^{-1}$ was prepared by a hypercritical drying method procedure (Utamapanya et al. 1991) and used for the degradation of dimethyl methylphosphonate (DMMP), a G agent simulant (Li and Klabunde 1991). The first mention of nanocrystalline MgO and CaO as stoichiometric reagents potentially usable for the decomposition of CWAs was published in 1996 (Klabunde et al. 1996). In the initial study, Wagner et al. (1999) described the decomposition of the solutions of sulfur mustard (HD), soman (GD) and VX at room temperature by nanostructured MgO which was listed as a reagent for the decontamination of sensitive components, military equipment and material. The mechanism for the decomposition of HD, GD and VX by nanocrystalline MgO (Wagner et al. 1999) and CaO (Wagner et al. 2000) is given in Fig. 2.

Nanocrystalline MgO decomposes HD into a mixture of divinylsulfide and thiodiglycol at a molar ratio of 1:1 (see Fig. 2). GD gives O-3,3-dimethyl-2-butyl methylphosphonic acid and methylphosphonic acid (see Fig. 2). Decomposition of VX leads to the formation of O-ethyl- methylphosphonic acid and methylphosphonic acid (see Fig. 2). In the decomposition of VX, it is important to avoid the toxic product S-2-diisopropyl(amino)ethyl-methyl phosphonothionate, E2192 (EA indicates that the agent is an experimental agent and is not actually in the U.S. arsenal). One of the products of the hydrolysis of VX in alkaline aqueous solution (Farquharson et al. 2005). As is evident from these diagrams, all three of these chemical substances, HD, GD and VX, decompose on the surface of MgO to form

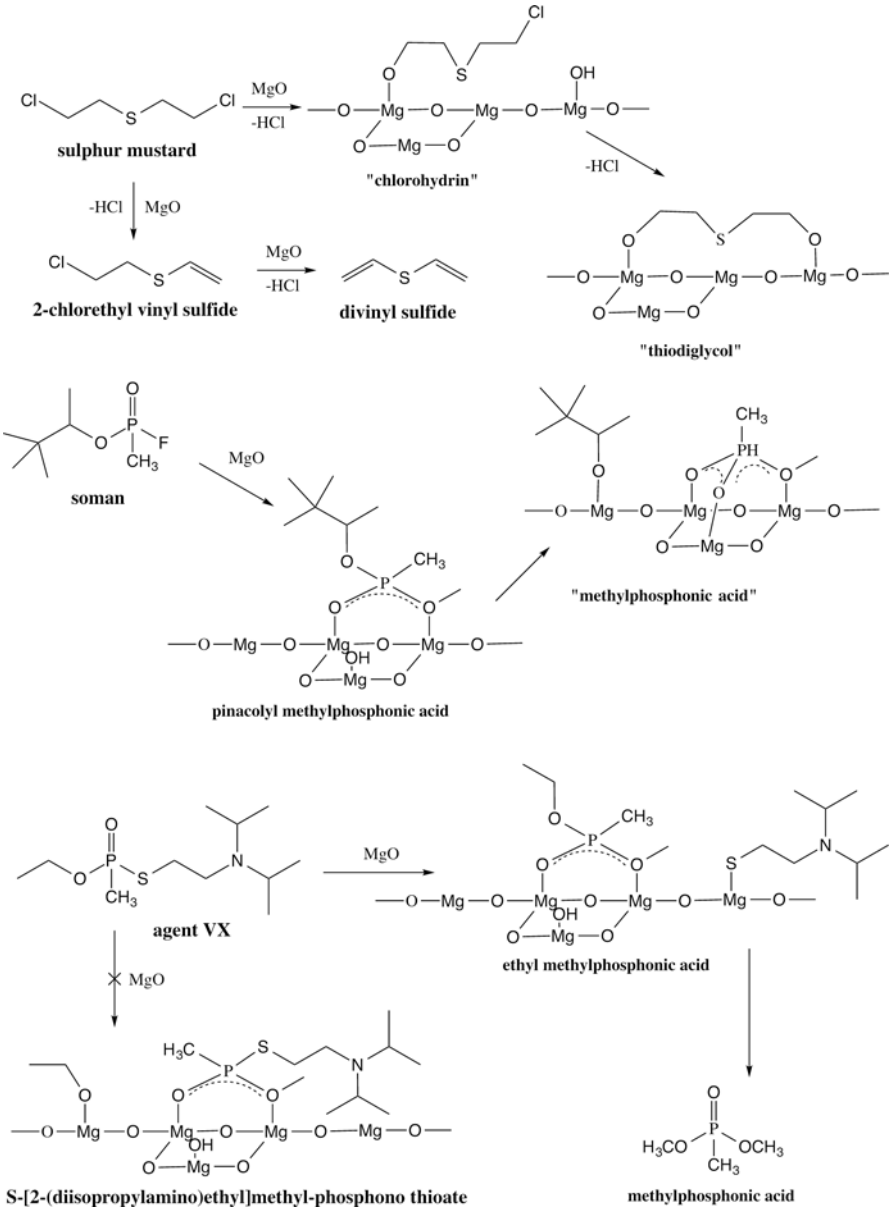

Fig. 2 Reaction scheme of the decomposition of HD, GD and VX on nanostructured MgO

non-hazardous products, which is very valuable for practical decontamination. Stengl et al. used an improved hypercritical drying method to prepare nanosized MgO with surface area greater than 1200 $m^2\ g^{-1}$ (Stengl et al. 2003). The highest percentage of the conversion of HD into harmless products after the completion of

the reaction was 77 % (Stengl et al. 2004). The particle morphology and texture of the material are also important factors that depend on its specific surface area and porosity. Another factor that influences the adsorption of molecules of chemical substances and their subsequent degradation on the material surface is the acid-base character of the surface. Tang et al. (2008) studied the effects of acidic and basic sites on the surface of CaO, MgO, SiO_2 and Al_2O_3 on the degradation of HD. According to their results, it can be concluded that the surfaces of the base-point oxides Al_2O_3, MgO and CaO exist regardless of whether the oxide is of generally acidic, basic or amphoteric character. Furthermore, it was observed (Tang et al. 2008) that oxides such as CaO and MgO have a large amount of strongly basic sites, but no acidic sites, and that Al_2O_3 is a typical amphoteric oxide with acidic and basic sites. Nazari and Nazari (2010) presented a simple and easily performed method for the synthesis of MgO particles and described the destruction of the CWAs simulants malathion (Diethyl 2[(dimethoxyphosphorothioyl) sulfanyl]butanedioate) and DMMP. It was also found that the decomposition of HD may be accelerated at the acid and basic sites. An increase in the degree of conversion of GD and VX by the nanostructured mixed oxide AlO(OH)•ZrO_2 (identified as sample AlZr_4) was caused by increasing the number of basic sites on the surface of the samples using a solution of NH_4OH, as presented in Fig. 3. The stoichiometric decomposition reaction (Klabunde et al. 1996) (unlike the photocatalytic reaction) is not dependent on exposure to light, but it is a surface-catalyzed hydrolysis reaction and involves the cleavage of chemical bonds. It should be noted that the macrocrystalline forms (particle size above 100 nm) of oxides of alkaline earth metals (Mg and Ca) and light metals (Al and Ti) (Wagner et al. 2007) have the ability to react with agents such as HD, GD and VX. However, the reactions on macrocrystalline oxides are generally slow and impractical for use in military decontamination.

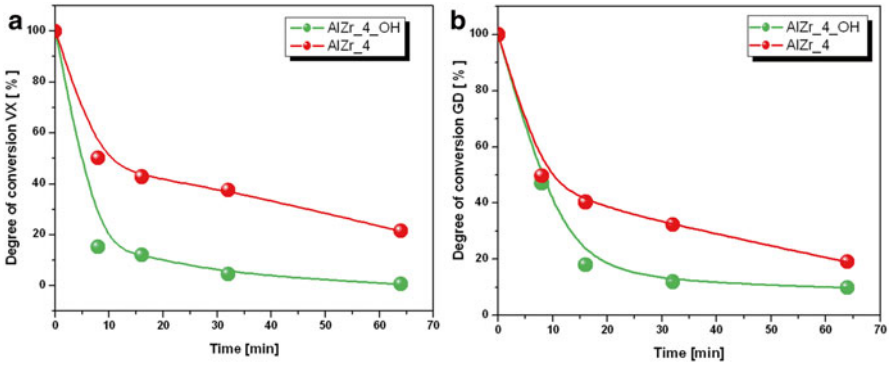

Fig. 3 The increase in conversion by increasing the number of basic sites (**a**) agent VX, (**b**) GD

2.2 Aluminum Oxide

Aluminum oxide is polymorphic. In its most common forms, it crystallizes as corundum, trigonal α-Al_2O_3, hexagonal β-Al_2O_3 and cubic γ-Al_2O_3. In nature, the monohydrate minerals boehmite γ -AlO(OH) and, rarely, diaspore α-AlO(OH) are formed, and the trihydrate gibbsite $Al(OH)_3 \cdot 3H_2O$ also forms. For decomposition of HD, GD and VX on nanocrystalline γ-Al_2O_3, TiO_2, metal titanium and aluminum (Štengl V et al. 2005) analogous degradation pathways have been suggested. Prasad et al. (2010) used alumina AP-Al_2O_3 and mixed alumina-transient metal oxide (AP-Al_2O_3–Fe_2O_3, AP-Al_2O_3–V_2O_5 and AP-Al_2O_3–CuO) prepared using an aerogel process (hypercritical drying procedure) for HD degradation. The value of the rate constant for HD degradation was determined to be 0.02 h^{-1} for alumina; for Al_2O_3–Fe_2O_3, Al_2O_3–V_2O_5 and Al_2O_3–CuO the values were 0.04, 0.03 and 0.03 h^{-1}, respectively. Nanoparticles of AP-Al_2O_3 in the size range 2–30 nm with a surface area of 375 m^2 g^{-1} were produced by the sol-gel method and were used for studying the kinetics of HD adsorption (Saxena et al. 2009).

2.3 Zinc Oxide

Zinc oxide (ZnO) crystallizes in two main structural forms, hexagonal wurtzite (Zn,Fe)S and cubic zincblende ZnS; in nature, crystalline zinc oxide occurs as the mineral zincite (Zn,Mn)O. Zinc oxide is widely used as an additive in numerous materials and products including plastics, ceramics, glass, cement, lubricants, paints, ointments, adhesives, sealants, pigments, batteries and fire retardants.

Prasad et al. used ZnO nanorods synthesized by a hydrothermal method (Prasad et al. 2007a) and ZnO from the sol-gel method (Mahato et al. 2009a) for HD and sarin degradation with rate constants of 0.36 h^{-1} and 0.08 h^{-1}, respectively. Houskova and Stengl (Houskovs et al. 2007; Houskova et al. 2007) prepared nanosized ZnO by homogeneous hydrolysis with thioacetamide heated at a temperature of 400 °C, which showed good decomposition of the HD, and its reactivity was superior to that of AP-MgO (Stengl et al. 2004). Mesoporous CuO-ZnO binary metal oxide was used as a decontaminant against HD (Kumar et al. 2013). These materials demonstrated superior decontamination properties against HD compared to single-component metal oxides and decomposed it to divinyl sulfide, chloroethyl vinyl sulfide and hemisulfur mustard.

2.4 Titanium Oxide

All three CWAs, i.e. neat HD, GD and VX, were hydrolyzed on the surface of TiO_2, and the reaction with VX is considerably rapid ($t_{1/2} < 30$ min) and approaches the rates attained in liquid decontaminant. Prasad et al. (2008) synthesized titania

nanotubes from anatase TiO_2 and NaOH under hydrothermal conditions at 130 °C for 5 days. The decontamination reaction of HD has a linear curve, with a fast initial reaction that reaches a steady state at later stages of the reaction with a rate constant of 0.1156 h^{-1} and a half-life of 5.99 h, thus indicating the pseudo first order behavior of the decontamination reaction of HD on TiO_2 nanotubes, whereas parent TiO_2 exhibited a rate constant of 0.0214 h^{-1} and a half-life of 32.39 h. Sarin reacted in a similar fashion: the rate of the decontamination reaction was found to be 0.7536^{-1} and the half-life was found to be 0.92 h; on bulk titania, the rate of the reaction was 0.0711 h^{-1} and the half-life of the reaction was 9.75 h. Ag^{+}-, Cu^{2+}-, Ni^{2+}-, CO_2^{+}-, Mn^{2+}- and Ru^{3+}-modified titania nanotubes have been studied as powder decontaminants against HD. Thiodiglycol and 1,4-oxathiane were observed to be the major products except on Ru^{3+}-titania nanotubes, where a sulfoxide of mustard formed, thereby indicating oxidative decontamination (Prasad et al. 2009).

Homogeneous hydrolysis of titanium oxo-sulfate has been used to prepare anatase TiO_2 with high specific surface area, and the degrees of conversion for HD, GD and VX into non-toxic products after the completion of the reaction for 64 min were 96.5 %, 96.6 % and 98.8 %, respectively (Štengl V et al. 2005).

2.4.1 Zr^{4+} and Hf^{4+}-Doped Titania

The homogeneous hydrolysis mixture of titanium oxo-sulfate and zirconium oxo-sulfate with urea at 98 °C was used to prepare Zr^{4+}-doped anatase with high specific surface area. During hydrolysis, complexes such as $[Zr(OH)n]^{4-n}$ could prevent the formation of crystalline particles and thus lead to gel precipitation. Good results were obtained for the decomposition of HD, where ~95 % conversion was achieved within 32 min. Total degradation of GD and VX on Zr-doped titania occurred in 1 min (Stengl et al. 2008; 2009). Doping TiO_2 with Hf (see Fig. 4) also increased the degradation rate of GD and VX. Figure 5 presents the kinetics of degradation of VX and GD on nanostructured Hf^{4+}-doped TiO_2; complete decomposition occurred at 30 s. The degree of conversion of HD is 85 % per h.

2.4.2 Ge^{4+} and In^{3+} Doped Titania

Germanium-doped TiO_2 was prepared by homogeneous hydrolysis of aqueous solutions of $GeCl_4$ and $TiOSO_4$ with urea. The best degrees of degradation, 100 % for GD, 99 % for VX and 95 % for HD, were achieved with samples with 2 wt.% germanium (Stengl et al. 2012a). Novel In^{3+}-doped TiO_2 and TiO_2/In_2S_3 nanocomposites for stoichiometric degradation of CWAs were prepared by homogeneous hydrolysis with urea and thioacetamide, respectively. The best degree of conversion for stoichiometric degradation of HD (98.5 %) occurred with In^{3+} doped titania containing 0.54 wt.% In (Stengl et al. 2012b).

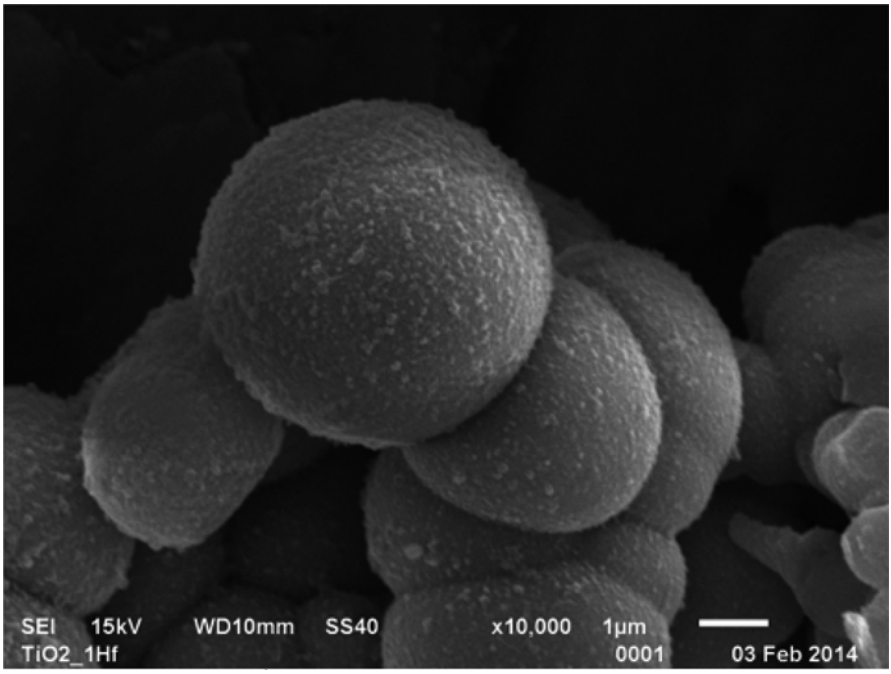

Fig. 4 SEM images of Hf $^{4+}$-doped TiO_2

2.4.3 Titania, Iron and Manganese Mixed Oxides

Titanium(IV)–manganese(IV) nanostructured mixed oxides were prepared by homogeneous hydrolysis of potassium permanganate and titanium(IV) oxo-sulfate with 2-chloroacetamide. The best decontamination properties for HD and GD were observed for the samples containing 18.7 % and 2.1 % Mn, where the degrees of conversion per h were 95.2 % and 89.3 %, respectively (Stengl et al. 2011b). Zirconium-doped mixed nanostructured oxides of Ti and Fe were prepared by homogeneous hydrolysis of iron and titania sulfate salts with urea in aqueous solution. The addition of Zr^{4+} to the hydrolysis of ferric sulfate with urea shifts the reaction route and promotes the formation of goethite FeO(OH) at the expense of ferrihydrite $Fe_5O_7(OH)•4H_2O$. The authors discovered that Zr^{4+}-doped oxo- hydroxides of Ti and Fe exhibit a higher degradation activity towards HD than any other yet- reported reactive sorbents. The reaction rate constant of the slower parallel reaction of the most efficient reactive sorbents is increased with an increasing amount of surface base sites (Stark and Klabunde 1996). Zirconium- doped nanostructured oxides of Fe, Al and Zn were prepared by homogeneous hydrolysis of the respective sulfate salts with urea in aqueous solution. The presence of Zr^{4+} dopant can increase both the surface area and the surface hydroxylation of the resulting doped oxides in addition to decreasing the crystallite size, thus potentially

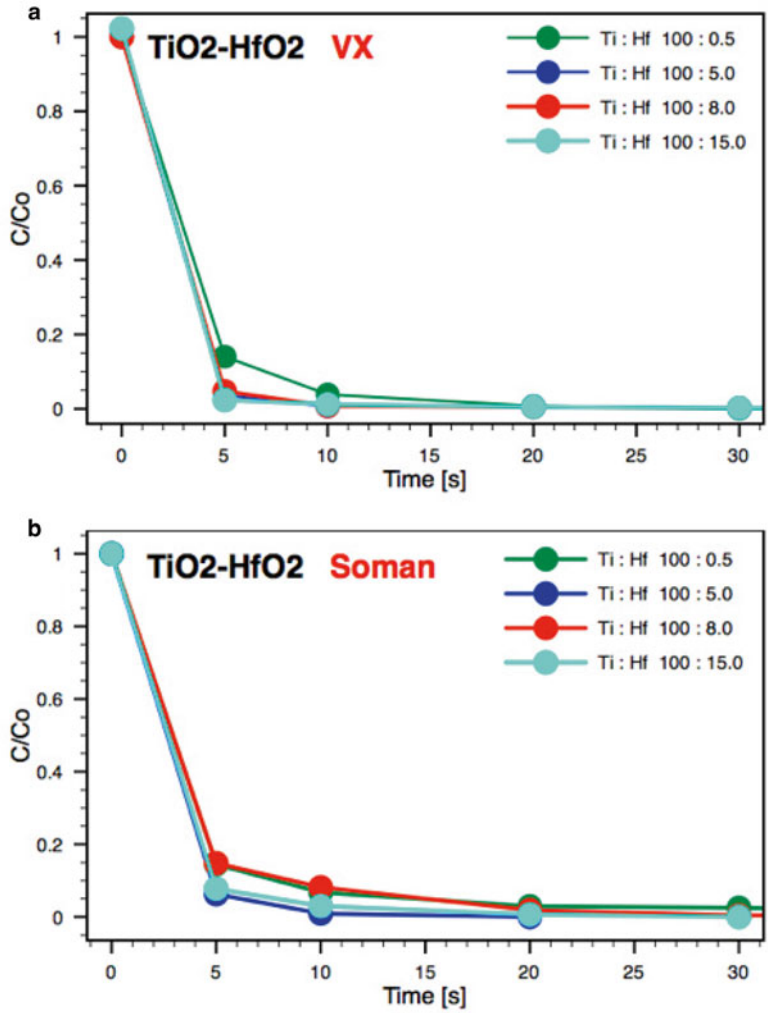

Fig. 5 Kinetics of degradation of (**a**) VX and (**b**) soman on Hf^{4+}-doped TiO_2 nanostructures

contributing to substrate adsorption at the oxide surface and thereby accelerating the rate of degradation of GD, HD, and VX. The addition of Zr^{4+} converts the product of the reaction of ferric sulfate with urea from ferrihydrite to goethite. We determined that the doped oxo-hydroxide Zr–FeO(OH) prepared by homogeneous hydrolysis of a mixture of ferric and zirconium oxo-sulfates in aqueous solution exhibit comparatively higher degradation activity towards CWAs. Degradation of GD or VX on Zr-doped FeO(OH) containing approximately 8.3 wt.% zirconium proceeded to completion within 30 min (Stengl et al. 2010).

Stengl et al. (2013) presented a procedure for the removal and detoxification of CWAs from corrosion-sensitive components using reactive sorption (adsorption

and bond cleavage). The procedure consists of spraying a suspended sorbent over a contaminated surface followed by the mechanical removal of the spent sorbent after evaporation of the liquid phase. The procedure was tested using a video graphics array (VGA) card, HD and a nanostructured Zr^{4+}—doped TiO_2 sorbent obtained by homogeneous hydrolysis. After allowing 60 min for a suspension of the reactive sorbent to react with the contaminated VGA card, 99.3 % of the HD was removed, while the VGA card retained its functionality. The procedure does not require specialized instrumentation and is feasible for electronic devices, as it does not need corrosive and electrically conducting agents or nonvolatile solvents that would harm electronic circuits. The method could be applicable for the decontamination of a broad range of CWAs and pesticides.

2.5 Zero-Valent Iron and Iron Oxides

Nanoscale zero-valent iron (Zboril et al. 2012) particles and a composite containing a mixture of ferrate(VI) and ferrate(III) were prepared by thermal procedures. Both nanoscale zero-valent iron and the ferrate(VI)/(III) composite removed HD completely; reactions of GD and VX with Fe(VI) were rapid, and complete degradation was achieved within 10 min. On the contrary, the efficiency of GD and VX degradation by nanoscale zero-valent iron was found to be below 50 % in a reaction time of ~1 h.

2.6 Zirconium Hydroxide

Commercial zirconium hydroxide (Mel Chemicals) was evaluated for its ability to detoxify CWAs GD, HD, and VX (Bandosz et al. 2012). The observed half-lives were 8.7 min, 2.3 h, and 1 min, respectively. The extraordinary reactivity of zirconium hydroxide toward VX is attributed to the complex chemistry associated with the surface of zirconia. The acidic bridging hydroxyl groups are proposed to protonate and hydrolyze VX in a manner analogous to ethyl methylphosphonic acid (EMPA) autocatalysis in solution.

2.7 Manganese Oxide (MnO_2)

Manganese(III, IV) oxide is a highly attractive inorganic material because of its physical and chemical properties and wide applications in catalysis, ion exchange, molecular adsorption bio sensors, and particularly, energy storage. Manganese(IV) oxide is polymorphic, with several different crystal structures such as α-MnO_2

(hollandite), β-MnO_2 (pyrolusite), δ-MnO_2 (birnessite), ε-MnO_2 (akhtenskite), γ-MnO_2 (nsutite) and amorphous MnO_2. Prasad et al. (2007b) used reactive sorbent based on nanosheets and nanotubes of manganese oxide for degradation of CEES with a rate constant of 0.148 h^{-1} and a half-life of 4.66 h, and for the detoxification of HD (Prasad et al. 2007c). Mesoporous manganese oxide MnO_2 nanobelts were prepared from Mn_2O_3 and NaOH by hydrothermal synthesis at 170 °C for 5 days. Decontamination reactions exhibited pseudo first order behavior, and the rate constant value and half-life were found to be 0.43 h^{-1} and 1.6 h, respectively, for GB; 0.01 h^{-1} and 69.32 h, respectively, for HD; and 0.02 h^{-1} and 34.66 h, respectively, for CEES (Mahato et al. 2010).

Manganese (IV) oxides were prepared by homogeneous hydrolysis of potassium permanganate with 2-chloroacetamide and direct reaction of potassium permanganate with manganese(II) sulfate in aqueous solution. The degree of conversion for HD and VX was very good for both samples and reached 95 % and 99 %, respectively. In contrast to HD and VX, degradation of GD was only 56 % on the cryptomelane-type MnO_2 and 18 % on the birnessite-type MnO_2 (Stengl et al. 2012c). The substituted iron(III)–manganese(III, IV) oxides ammoniojarosite (NH_4)$Fe_3(SO_4)_2(OH)_6$ and birnessite $K(Mn^{4+},Mn^{3+})_2O_4$ were prepared by homogeneous hydrolysis of potassium permanganate and iron(III) sulfate with 2-chloroacetamide and urea, respectively. The best activities for the degradation of HD (97.9 % in 64 min) and GD (97.9 % in 64 min) were observed for FeMn_75, which contained 32.6 wt.% Fe (36.8 wt.% Mn) and FeMn_37U, which contained 60.8 wt.% Fe (10.1 wt.% Mn), respectively (Stengl et al. 2012d).

2.8 Vanadium Oxide

Mahato et al. (2009b) synthesized nonstoichiometric $V_{1.02}$O2.98 nanotube samples from vanadium pentoxide and dodecyl amine under hydrothermal conditions at 180 °C for 7 days. The values of the kinetic rate constants for HD and GB degradation were calculated to be 0.11 and 0.1 h^{-1}. The products of the HD degradation were mustard sulfoxide and thiodiglycol, and GB gave isopropyl methylphosphonic acid. The results show that the nanostructure of $V_{1.02}O_{2.98}$ permits promising oxidative and hydrolysis reactions comparable with the existing solid decontamination systems such as nanosized MgO and Al_2O_3. Degradation of HD and its simulant 2-chloroethyl ethyl sulfide (CEES) were investigated on the surface of porous vanadium $_{oxide}$ VO_x nanotubes at room temperature; the study explored the roles of hydrolysis, elimination and oxidation reactions in the detoxification of HD and CEES, and the first order rate constant and t1/2 were calculated to be 0.026 h^{-1} and 26.6 h, respectively, for CEES and 0.052 h^{-1} and 13.24 h, respectively, for HD (Singh et al. 2011).

2.9 Ce^{3+} and Ce^{4+} Oxides

Cerium oxide belongs to the most important category of rare earths with numerous applications in such diverse areas as catalysis, (Wang and Lin 2004) fuel cell systems, (Babu et al. 2012) and glass polishing (Janoš and Petrák 1991). Crystalline cerium(IV) oxide exhibits a characteristic face-centered cubic (fluorite-type) structure, which is not disturbed by the presence of other lanthanides in concentrations of up to ca. 50 %. Typically, a portion of the Ce atoms exist in a reduced (trivalent) state in cerium(IV) oxide. The ability of Ce to switch between the two oxidation states is related to the unique catalytic activity and versatile applicability of cerium oxide. In recent times, cerium oxide has gained a great deal of attention because of its ability to interact with phosphate ester bonds in biologically relevant molecules including ATP and DNA. Currently, it is regarded as one of the most promising artificial enzymes, also called nanozymes (Wei and Wang 2013). These unique properties (enhanced catalytic activity, enzyme-mimetic ability) are usually attributed to the specifically designed nano-sized forms of cerium dioxide, nanoceria. The ability of cerium oxide to destroy dangerous organophosphate compounds has been discovered only recently (Janoš et al. 2014). Ceria-based reactive sorbents were effective in the degradation of organophosphate pesticides (parathion-methyl, chlorpyrifos, dichlofenthion, fenchlorphos, and prothiofos) and of some CWAs (the nerve gases GD and VX) under relatively mild conditions at ambient temperature. A highly reactive sorbent may be prepared not only from pure Ce compounds but also from cerium concentrates containing a certain amount of other lanthanides, and even from spent ceria-based glass-polishing sludges (Janoš submitted) (see Fig. 6).

Many synthetic routes have been used to prepare the catalytically active forms of nano-ceria, including sol-gel methods, thermolysis and homogeneous hydrolysis. It was shown that conventional precipitation/calcination methods may be adopted to produce ceria-based reactive sorbents with excellent degradation efficiency; a simple and easily scalable procedure involves the precipitation of sparingly soluble cerium carbonate (either with an ammonium bicarbonate solution or with a gaseous mixture of CO_2 and NH_3) with subsequent calcination in the presence of oxygen (air) (Janoš and Petrák 1991; Janoš et al. 2014; Janoš submitted). The properties of cerium oxide, such as its specific surface area, crystallinity, Ce^{3+}/Ce^{4+} ratio, the presence of surface functional groups and its reactivity with organophosphate compounds, may be finely tuned by the proper selection of calcination conditions.

It was suggested that organophosphate degradation in the presence of cerium oxide is governed by the S_N2 mechanism, a nucleophilic substitution in which the –OH groups on the sorbent surface attack the P atom in the organophosphate molecule. It was confirmed that the formation of the –OH groups is energetically favorable, especially in the vicinity of oxygen vacancies associated with the presence of non-stoichiometric "impurities", such as Ce^{3+} cations (Hayun et al. 2011). In accordance with the proposed reaction mechanism, the organophosphate

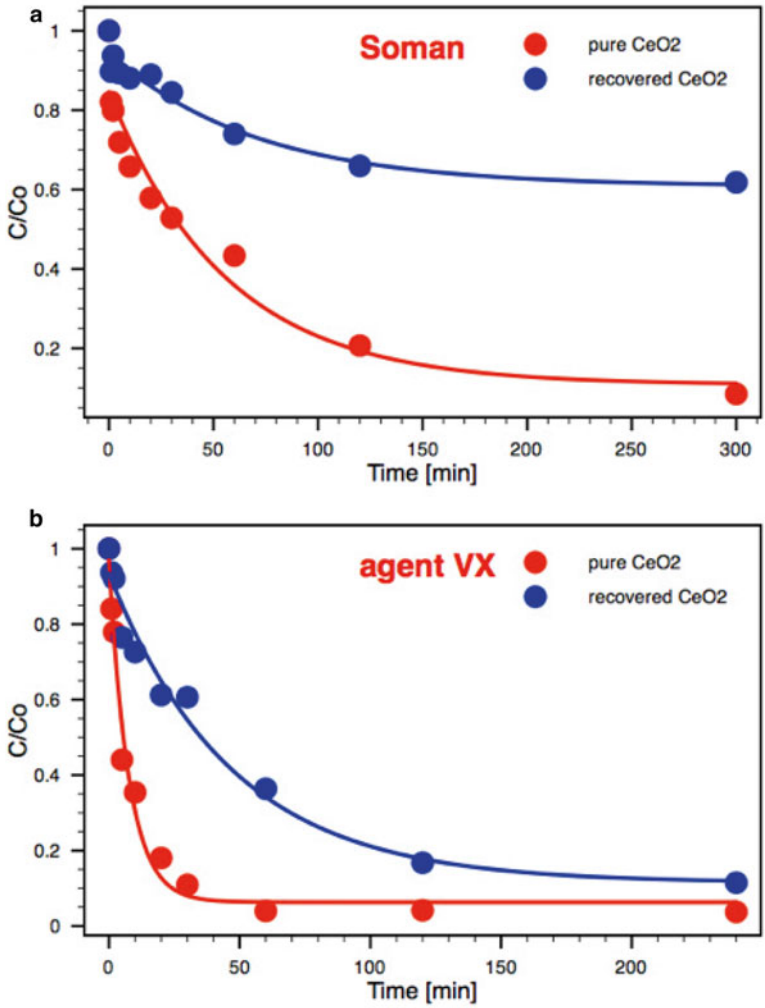

Fig. 6 Degradation of soman (**a**) and VX (**b**) on pure CeO_2 and on CeO_2 recovered from spent glass polishing slurry. Nonane was used as the reaction medium

degradation is promoted in aprotic solvents. As shown in Fig. 6, the almost complete degradation of VX was achieved in nonane within approximately 1 h (Janoš submitted). Both non-polar solvents (heptane, nonane) and polar aprotic solvents (acetonitrile, acetone) that are miscible with water can be used as reaction media (Janoš et al. 2014). This opens new possibilities for designing more versatile decontamination strategies.

Cerium oxide prepared from a carbonate precursor consists of relatively large clusters of irregularly shaped thin plates with diameters of several micrometers.

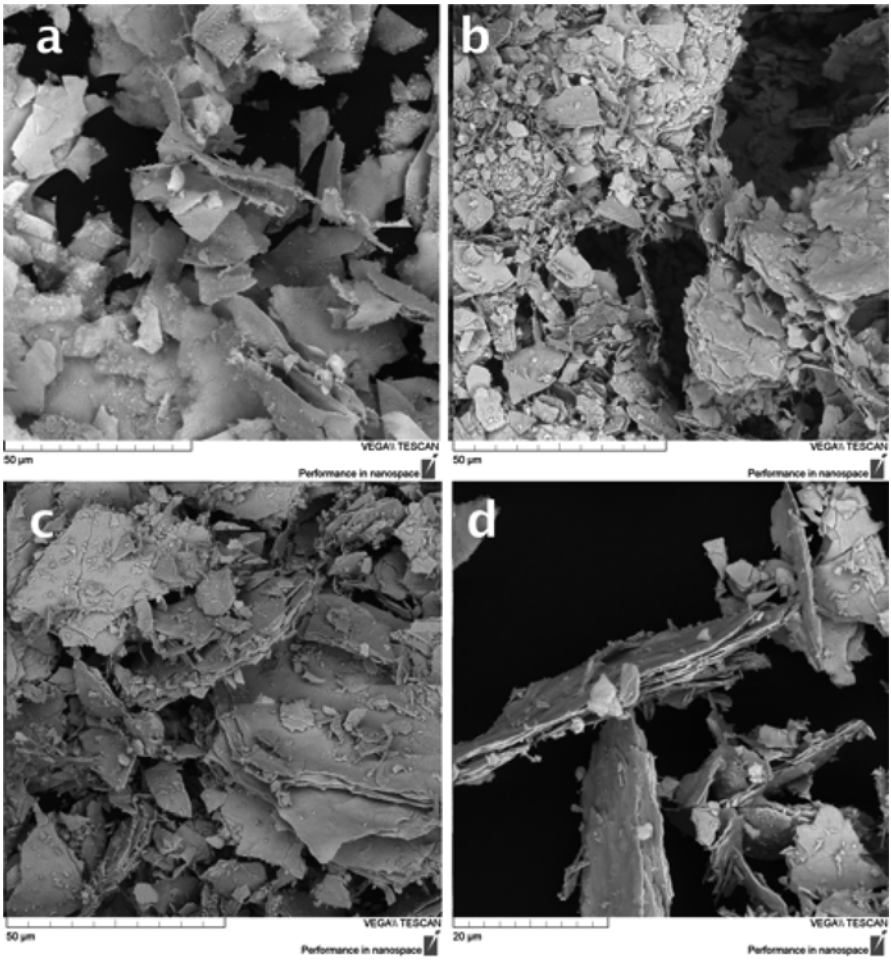

Fig. 7 SEM images of (**a**) cerium carbonate (precursor); (**b**) cerium oxide annealed at 500 °C; (**c**) cerium oxide doped with 5 % La; (**d**) cerium oxide doped with 5 % Pr

The characteristic layered structure of cerium oxide (with plate thickness on the order of nanometers), which is most likely a reason for its high degradation efficiency, is clearly visible in Fig. 7. The presence of minor amounts of other lanthanides (up to 5 % of La, Nd, and Pr, expressed as the respective oxides) does not significantly affect the physico-chemical properties or the degradation efficiency of cerium oxide (Janoš et al. 2014). Thus, relatively impure and low-cost cerium concentrates may be used for preparing effective reactive sorbents. A comparison of reactive sorbents based on nanostructured oxides for the stoichiometric degradation of HD is presented in Table 1.

Table 1 Comparing the effectiveness of selected reactive sorbents for sulfur mustard stoichiometric degradation for time degradation reaction 64 min

Reactive sorbents	Method of preparation	Degree of conversion 64 min [%]	k [s^{-1}]	k_1 [s^{-1}]	k_2 [s^{-1}]	Reference
MgO	Aerogel	68.0	5×10^{-4}		–	Stengl et al. (2004)
TiO_2-anatase	Urea hydrolysis	96.5	3.1×10^{-3}	–	–	Štengl et al. (2005)
Zn doped TiO_2	Urea hydrolysis	98.7	3.3×10^{-3}	–	–	Houskovs et al. (2007)
Zr doped TiO_2[a]	Urea hydrolysis	96.0	–	1.4×10^{-1}	$2–6\times10^{-3}$	Stengl et al. (2009)
In doped TiO_2	urea hydrolysis	98.5	–	2.2×10^{-2}	7.1×10^{-4}	Stengl et al. (2012b)
Ge doped TiO_2	Urea hydrolysis	97.7	–	1.9×10^{-1}	1.2×10^{-3}	Stengl et al. (2012a)
ferrihydrite	Urea hydrolysis	83.5	2.5×10^{-3}	–	–	Štengl et al. (2005)
Fe-Zr mixed oxides	Urea hydrolysis	95.0	5.1×10^{-3}	–	–	Stengl et al. (2010)
Al-Zr mixed oxides	Urea hydrolysis	74.0	1.9×10^{-3}	–	–	Stengl et al. (2010)
Zn-Zr mixed oxides	Urea hydrolysis	47.7	8.9×10^{-4}	–	–	Stengl et al. (2010)
Ti-Fe-Zr mixed oxides	Urea hydrolysis	99.5	–	4.5×10^{-2}	9.9×10^{-4}	Stengl et al. (2011a)
α-MnO_2	Chloroacetamide hydrolysis	95.1	–	1.4×10^{-2}	3.5×10^{-3}	Stengl et al. (2012c)
δ-MnO_2	Chloroacetamide hydrolysis	95.8	2.3×10^{-3}	–	–	Stengl et al. (2012c)
Ti-Mn mixed oxides	Chloroacetamide hydrolysis	95.2	–	4.7×10^{-2}	2.1×10^{-3}	Stengl et al. (2011b)
Mn-doped jarosite	Chloroacetamide hydrolysis	95.5	–	2.6×10^{-2}	3.9×10^{-4}	Stengl et al. (2012d)
Fe doped MnO_2	Chloroacetamide hydrolysis	97.8	–	1.4×10^{-0}	1.5×10^{-3}	Stengl et al. (2012d)
TiO_2-GeS_2	Thioacetamide hydrolysis	96.4	–	3.7×10^{-1}	6.7×10^{-4}	Stengl et al. (2012a)
TiO_2-In_2S_3	Thioacetamide hydrolysis	96.7	–	3.5×10^{-2}	1.1×10^{-3}	Stengl et al. (2012b)

[a]Time of degradation reaction 32 min

3 Conclusions

Further research is necessary to search for new, alternative and advanced technologies for CWA decontamination applications using nanostructured transient metal oxides. Previous work has shown that in many cases, the nanostructured metal oxides operate rather selectively and decompose each of the well-known types of warfare agents (HD, GD, GB, VX) with relatively good efficiency. Additional research in the field of nanostructured materials should focus on new materials for the degradation of CWAs with other chemical structures such as cyanophosphonates (tabun), agents containing an arsenic atom (lewisite, adamsite), new compounds based on phosphates (Novichok agents), derivatives of fentanyl and highly toxic halogenated oximes (phosgene oxime). New composite materials based on nanostructured transition metal oxides with graphene, carbon nanotubes or fullerenes have shown promise. In the future, these materials may become the basis for protective "self-decontaminating" materials to protect military equipment from the effects of toxic chemical and biological agents and to significantly facilitate and accelerate decontamination interventions.

Acknowledgements This work was supported by RVO 61388980 and the Czech Science Foundation (Project No. P106/12/1116).

References

Babu KS, Arunkumar P, Meena M (2012) A review on cerium oxide-based electrolytes for ITSOFC. Nanomat Energy 1:288

Bandosz TJ, Laskoski M, Mahle J, Mogilevsky G, Peterson GW, Rossin JA, Wagner GW (2012) Reactions of VX, GD, and HD with Zr(OH)4: Near instantaneous decontamination of VX. J Phys Chem C 116:11606

Farquharson S, Gift A, Maksymiuk P, Inscore F (2005) Surface-enhanced Raman spectra of VX and its hydrolysis products. Appl Spectrosc 59:654

Hayun S, Shvareva TY, Navrotsky A (2011) Direct measurement of surface energy of CeO_2 by differential scanning calorimetry. J Am Ceram Soc 94:3992

Houskova V, Stengl V, Bakardjieva S, Murafa N, Kalendova A, Oplustil F (2007) Nanostructure materials for destruction of warfare agents and eco-toxins prepared by homogeneous hydrolysis with thioacetamide: Part 1—zinc oxide. J Phys Chem Solids 68:716

Houskovs V, Stengl V, Bakardjieva S, Murafa N, Kalendova A, Oplustil F (2007) Zinc oxide prepared by homogeneous hydrolysis with thioacetamide, its destruction of warfare agents, and photocatalytic activity. J Phys Chem A 111:4215

Janoš P, Kuran P, Ederer J, Stastny M, Toman P, Psenicka M, Mazanec K, Skoumal M. J Rare Earth, submitted

Janoš P, Petrák M (1991) Preparation of ceria-based polishing powders from carbonates. J Mater Sci 26:4062

Janoš P, Kuran P, Kormunda M, Stengl V, Grygar TM, Dosek M, Stastny M, Ederer J, Pilarova V, Vrtoch L (2014) Cerium dioxide as a new reactive sorbent for fast degradation of parathion methyl and some other organophosphates. J Rare Earth 32:360

Khaleel A, Lucas E, Pates S, Koper OB, Klabunde KJ (1999) Nanocrystals as destructive adsorbents for chemical agents, biological agents, and air pollutants. Abstr Pap Am Chem S 217:U591

Klabunde KJ, Stark J, Koper O, Mohs C, Park DG, Decker S, Jiang Y, Lagadic I, Zhang D (1996) Nanocrystals as stoichiometric reagents with unique surface chemistry. J Phys Chem 100:12142

Koper OB, Lagadic I, Volodin A, Klabunde KJ (1997) Alkaline-earth oxide nanoparticles obtained by aerogel methods. Characterization and rational for unexpectedly high surface chemical reactivities. Chem Mater 9:2468

Kumar JP, Prasad GK, Ramacharyulu PVRK, Garg P, Ganesan K (2013) Mesoporous CuO-ZnO binary metal oxide nanocomposite for decontamination of sulfur mustard. Mater Chem Phys 142:484

Li YX, Klabunde KJ (1991) Nanoscale metal-oxide particles as chemical reagents—destructive adsorption of a chemical-agent simulant, dimethyl methylphosphonate, on heat-treated magnesium-oxide. Langmuir 7:1388

Lucas E, Decker S, Khaleel A, Seitz A, Fultz S, Ponce A, Li W, Carnes C, Klabunde KJ (2001) Nanocrystalline metal oxides as unique chemical reagents/sorbents. Chem Eur J 7:2505

Mahato TH, Prasad GK, Singh B, Acharya J, Srivastava AR, Vijayaraghavan R (2009a) Nanocrystalline zinc oxide for the decontamination of sarin. J Hazard Mater 165:928

Mahato TH, Prasad GK, Singh B, Srivastava AR, Ganesan K, Acharya J, Vijayaraghavan R (2009b) Reactions of sulphur mustard and sarin on V1.02O2.98 nanotubes. J Hazard Mater 166:1545

Mahato TH, Prasad GK, Singh B, Batra K, Ganesan K (2010) Mesoporous manganese oxide nanobelts for decontamination of sarin, sulphur mustard and chloro ethyl ethyl sulphide. Micropor Mesopor Mat 132:15

Nazari B, Jaafari M (2010) A new method for the synthesis of MgO nanoparticles for the destructive adsorption of organophosphorus compounds. Dig J Nanomater Bios 5:909

Prasad GK, Mahato TH, Singh B, Ganesan K, Pandey P, Sekhar K (2007a) Detoxification reactions of sulphur mustard on the surface of zinc oxide nanosized rods. J Hazard Mater 149:460

Prasad GK, Mahato TH, Pandey P, Singh B, Suryanarayana MVS, Saxena A, Shekhar K (2007b) Reactive sorbent based on manganese oxide nanotubes and nanosheets for the decontamination of 2-chloro-ethyl ethyl sulphide. Micropor Mesopor Mat 106:256

Prasad GK, Mahato TH, Singh B, Pandey P, Rao AN, Ganesan K, Vijayraghavan R (2007c) Decontamination of sulfur mustard on manganese oxide nanostructures. AIChE J 53:1562

Prasad GK, Mahato TH, Singh B, Ganesan K, Srivastava AR, Kaushik MP, Vijayraghavan R (2008) Decontamination of sulfur mustard and sarin on titania nanotubes. AIChE J 54:2957

Prasad GK, Singh B, Ganesan K, Batra A, Kumeria T, Gutch PK, Vijayaraghavan R (2009) Modified titania nanotubes for decontamination of sulphur mustard. J Hazard Mater 167:1192

Prasad GK, Ramacharyulu PV, Batra K, Singh B, Srivastava AR, Ganesan K, Vijayaraghavan R (2010) Decontamination of Yperite using mesoporous mixed metal oxide nanocrystals. J Hazard Mater 183:847

Saxena A, Sharma A, Srivastava AK, Singh B, Gutch PK, Semwal RP (2009) Kinetics of adsorption of sulfur mustard on Al_2O_3 nanoparticles with and without impregnants. J Chem Technol Biot 84:1860

Sayle DC, Seal S, Wang Z, Mangili BC, Price DW, Karakoti AS, Kuchibhatla SV, Hao Q, Mobus G, Xu X, Sayle TX (2008) Mapping nanostructure: a systematic enumeration of nanomaterials by assembling nanobuilding blocks at crystallographic positions. ACS Nano 2:1237

Singh B, Mahato TH, Srivastava AK, Prasad GK, Ganesan K, Vijayaraghavan R, Jain R (2011) Significance of porous structure on degradation of 2,2' dichlorodiethyl sulphide and 2 chloroethyl ethyl sulphide on the surface of vanadium oxide nanostructure. J Hazard Mater 190:1053

Stark JV, Klabunde KJ (1996) Nanoscale metal oxide particles/clusters as chemical reagents. Adsorption of hydrogen halides, nitric oxide, and sulfur trioxide on magnesium oxide nanocrystals and compared with microcrystals. Chem Mater 8:1913

Stark JV, Park DG, Lagadic I, Klabunde KJ (1996) Nanoscale metal oxide particles/clusters as chemical reagents. Unique surface chemistry on magnesium oxide as shown by enhanced adsorption of acid gases (sulfur dioxide and carbon dioxide) and pressure dependence. Chem Mater 8:1904

Stengl V, Bakardjieva S, Marikova M, Bezdicka P, Subrt J (2003) Magnesium oxide nanoparticles prepared by ultrasound enhanced hydrolysis of Mg-alkoxides. Mater Lett 57:3998

Stengl V, Bakardjieva S, Marikova M, Subrt J, Oplustil F, Olsanska M (2004) Aerogel nanoscale magnesium oxides as a destructive sorbent for toxic chemical agents. Cent Eur J Chem 2:16

Štengl V, Marikova M, Bakardjieva S, Subrt J, Oplustil F, Olsanska M (2005) Reaction of sulfur mustard gas, soman and agent VX with nanosized anatase TiO_2 and ferrihydrite. J Chem Technol Biot 80:754

Stengl V, Bakardjieva S, Murafa N, Oplustil F (2008) Zirconium doped titania: destruction of warfare agents and photocatalytic degradation of orange 2 dye. Open Proc Chem J 1:1

Stengl V, Bakardjieva S, Murafa N, Oplustil F, Osterlund L, Mattsson A, Andersson PO (2009) Warfare agents degradation on zirconium doped titania. Microsc Microanal 15:1038

Stengl V, Houskova V, Bakardjieva S, Murafa N, Marikova M, Oplustil F, Nemec T (2010) Zirconium doped nano-dispersed oxides of Fe, Al and Zn for destruction of warfare agents. Mater Charact 61:1080

Stengl V, Grygar TM, Oplustil F, Nemec T (2011a) Sulphur mustard degradation on zirconium doped Ti-Fe oxides. J Hazard Mater 192:1491

Stengl V, Bludska J, Oplustil F, Nemec T (2011b) Mesoporous titanium-manganese dioxide for sulphur mustard and soman decontamination. Mater Res Bull 46:2050

Stengl V, Grygar TM, Oplustil F, Nemec T (2012a) Ge^{4+} doped TiO_2 for stoichiometric degradation of warfare agents. J Hazard Mater 227:62

Stengl V, Oplustil F, Nemec T (2012b) In^{3+}-doped TiO_2 and TiO_2/In_2S_3 nanocomposite for photocatalytic and stoichiometric degradations. Photochem Photobiol 88:265

Stengl V, Kralova D, Oplustil F, Nemec T (2012c) Mesoporous manganese oxide for warfare agents degradation. Micropor Mesopor Mat 156:224

Stengl V, Grygar TM, Bludska J, Oplustil F, Nemec T (2012d) Mesoporous iron-manganese oxides for sulphur mustard and soman degradation. Mater Res Bull 47:4291

Stengl V, Grygar TM, Oplustil F, Olsanska M (2013) Decontamination of sulfur mustard from printed circuit board using Zr-doped titania suspension. Ind Eng Chem Res 52:3436

Tang H, Cheng Z, Zhu H, Zuo G, Zhang M (2008) Effect of acid and base sites on the degradation of sulfur mustard over several typical oxides. Appl Catal B-Environ 79:323

Utamapanya S, Klabunde KJ, Schlup JR (1991) Nanoscale metal-oxide particles clusters as chemical reagents—synthesis and properties of ultrahigh surface-area magnesium-hydroxide and magnesium-oxide. Chem Mater 3:175

Wagner GW, Bartram PW, Koper O, Klabunde KJ (1999) Reactions of VX, GD, and HD with nanosize MgO. J Phys Chem B 103:3225

Wagner GW, Koper OB, Lucas E, Decker S, Klabunde KJ (2000) Reactions of VX, GD, and HD with nanosize CaO: autocatalytic dehydrohalogenation of HD. J Phys Chem B 104:5118

Wagner GW, Procell LR, Munavalli S (2007) (27)AI, Ti-47,Ti-49, P-31, and C-13 MAS NMR study of VX, GD, and HD reactions with nanosize Al_2O_3, conventional Al_2O_3 and TiO_2, and aluminum and titanium metal. J Phys Chem C 111:17564

Wang C-H, Lin S-S (2004) Preparing an active cerium oxide catalyst for the catalytic incineration of aromatic hydrocarbons. Appl Catal A-Gen 268:227

Wei H, Wang E (2013) Nanomaterials with enzyme-like characteristics (nanozymes): next-generation artificial enzymes. Chem Soc Rev 42:6060

Yang YC, Baker JA, Ward JR (1992) Decontamination of chemical warfare agents. Chem Rev 92:1729

Zboril R, Andrle M, Oplustil F, Machala L, Tucek J, Filip J, Marusak Z, Sharma VK (2012) Treatment of chemical warfare agents by zero-valent iron nanoparticles and ferrate(VI)/(III) composite. J Hazard Mater 211–212:126